Industry Nexus, Volume 1, Issue 1 (2025), 1-15

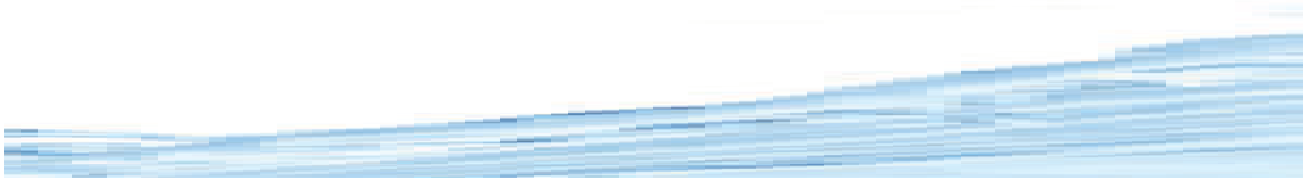

Characterization of hydro mechanical deep drawing process on multi-layer alloy sheet using polyurethane ring by thermal gradients and water jet injection

Gunasekar P [1], Anderson A [2]

[1] Saveetha School of Engineering, Saveetha Institute of Medical and Technical Sciences, Chennai, India)

[2] Department of Mechanical Engineering, Sathyabama institute of science and Technology, Sholinganallur, Chennai-600119

(Received 12 December 2024; Revised 12 February 2025; accepted 05 March 2025)

Abstract

The HMDD process is implemented to improve the forming conditions of the metals such as aluminium and magnesium alloys. In this paper, we consider the application of hydro-mechanical deep drawing (HMDD) process on the multilayer aluminium/steel laminated sheets by means of experiment and finite element (FE) method. In addition, this paper also investigates the effects of isothermal gradient on formability of multilayer sheets using cup drawing tool and drawing efficiency of polyurethane ring. The multilayer layup laminate such as aluminium/steel/aluminium (A1) and steel/aluminium/steel (S1) are tested for the different properties both experimentally and numerically. The sheet A1 and S1 are joined together by the typical welding process. During the deep drawing process, there is a high possibility of irregular thickness distribution. Hence, the thickness effect must be taken into account in 3D finite element simulation. The water is injected by jet to cool the draw cup wall. To verify the results, the multilayer sheet solved numerically and compared with the experimental dynamic analysis. Using the analytical model created by Kim and developed FE model, the parameters like the effect of limiting drawing ratio, formability improvement on materials, effect of punch force and hydraulic pressure, layer thickness and layer arrangement effect and vibration due to punching studied in detail. From the results it is found, the formability of the material is high in isothermal condition compared to non-isothermal. By warming the tool, the formability is improved 20% on non-isothermal condition. Further, the wider working zone is possible for a multi-layer sheet by decreasing the drawing ratio and the thickness of the sheet. The punch force and the pressure required on the non-isothermal is 5% higher than isothermal forming. The natural frequencies are measured for forming simulations, higher the frequencies higher error owing to high intense material flow.

Keywords: Green buildings, green strategies, energy conservation, LEED certification, rating system.

Email address for correspondence: konguguna@gmail.com

1.**Introduction**

The deep drawing process is a technique which is widely spreading now days. It is used to form simple and complex components using a blank sheet. They possess numerical production applications such as cup, cans, box, vessels and many others[1]. The blank sheet placed on a blank holder followed by rigid tool called die. The pressure is applied on the punch to form a desired shape. During formation of shape, thinning and thinking occurs and estimating them is very challenging [2–4]. Formability of the shape which is made of two or more laminated structures is another key area of research. The application of the multilayer materials is very significant. In recent years much attention paid on multi layer sheets owing to industrial demands. The multi layer sheets are joined together for forming process due to its better mechanical property and failure theories using process such welding, roll bonding and adhesive bonding. Compared to above, welding and bonding found in wide applications, although they are not corrosion resistance. The corrosion resistance coating is done above the welded area. Even though the properties of the corrosion are not significant however, the welded process good in wear resistance and electrical conductivity. The parameters like punch speed, forming temperature, blank metal and tool geometry only decided the quality of deep drawing. There are various technique used to find limit curve. However, Erishen cup test is widely used to evaluate the formability of sheet material [5]. During formation of the cup, generation of noise is unavoidable. The noise and vibration is formed when the punch hit the blank is very disturbing to the environment. In addition to the other characteristics, study of vibration is vital due to its restrictive regulations in both noise and vibrations. The study of vibration and vibroacoustic simulations is an important aspect in many industries like aerospace, automobile etc [6]. Form the aforementioned statement, the estimation of the vibro-acoustic parameters is important. Manigandan et al studied the effects of noise in the near and far field. The noise and vibration creates the discomfort to the nearby's [7]. There are abundant study is available on deep drawing process in last few years. However, study on aero acoustic vibration is very limited. The low weight Al-sheet commonly used in light weight applications. Although they have plenty of applications, the formability of the sheets is very poor in non isothermal condition owing to high flow stress and deformation. Hence warm forming is suggested to overcome those difficulties by allowing the deeper drawing and good stretching [8]. Early study found, the enhancement of LDR can increase the formability by 9% and 10% in Al-Mg sheet. The elongation increased approximately 200-350% for warm deep drawing [9]. To avoid complexity in carrying out experimental project, FE is used for warm forming process. The designed analytical model is proposed based on few variables such as tool geomentry, blank material, punch force, anisotropy and friction [10,11]. Notable studied observed the experimental results are reasonably in good argument with FE simulations[12–14]. The warm and cold results are compared to find the LDR and formability strength. Due to the better property, two layer sheets and bimetallic sheets gained a shining attention among the researchers. Parsa et al. investigated the two layers Aluminium/ Stainless steel sheets both numerically and experimentally. They found the Al/Steel sheets results in better drawing ratio than Steel/ Al [5]. Similarly, Baghezadeh et al. demonstrated the hydro mechanical deep drawing process on Al/Steel sheets. They also carried same results in thickness ratio and formability. The higher LDR is achievable in A/S layup from S/A layup[14]. Mayavan et al studied the behaviour of bimetallic 513 CR3 steel sheets for comparing the thickness in various regions by limiting drawing ratio. The simulation done using Abaqus 6.12 and Kim analytical model [15]. The finding is reasonable compared to literatures [16]. Tseng et al studied the formability of two layer (Al/Cu) sheet through FE simulations and experiment[6]. The dual layer sheet is fabricated using roll bonding process. They found the formability of monolithic sheet is pretty higher than bilithic layer sheets. The prediction of the formability is improved by Jalali et al, by introducing new theoretical model[17]. They demonstrated the limiting drawing for 2 layer sheet between the materials. Maleki et al studied thickness and bonding strength of the Al/Steel layer sheet. They found the yield strength and thickness reduction is due to the bonding strength [18].

In previous finding, the formability is improved by varying the LDR and bonding type. Lang et al. conducted the experiment in one layer sheet using HMDD process. They found implementation of HMDD increases the formability of the blank into useful structure. The radial pressure is assisted with HMDD process to produce better drawing ratio [19]. Fazil & Dariani also investigated the formability in HMDD assistance. They found, HMDD process is very vital to reach higher drawing ratio than conventional deep drawing [20]. Plenty of notable works done by several researchers on HMDD. Rahmani et al studied the working zone of square cups[21]. Decreasing friction between the sheets and holder results in larger working zone and better drawing ratio. Choi et al predicted the wrinkling on the monolithic asymmetric sheet. They found the formability depends on parameters like fluid pressure, punch force and punch speed [22]. Zhang et al., investigated the

multilayer sheets, the top and bottom layer made of steel with middle layer thin aluminium sheet[23] . The formability of thin Al layer is studied and found friction coefficients. The friction coefficient determines the formability of the structure. Even though several study is carried out on multilayer sheet and bimetalic sheet in presence of HMDD. The study of multilayer sheet with HMDD on vibration acoustic is very limited. In this research, 3D finite simulation is carried out with HMDD and isothermal process of multilayer sheet using abaqus. The common code is incorporated in user defined subroutine to solve the problem in dynamic explicit method. The pressure applied on the blank is non uniform. The parameters like effect of temperature gradient in forming, forming force, thickness distribution, LDR prediction and vibration acoustic is formed using FE and compared with experimental model.

2. Experimental description

The study in this paper is concerning wide application of Al/Steel laminated sheets which is fabricated in form of multilayer sheet along with polyurethane ring. Two layers of steel and one layer of Al joined to make a specimen S1. Likewise, the specimen 2 is made of two layer of aluminium to one layer of steel for A1. The base material is ST13 (Steel) and AA1050 (aluminium alloy) was fabricated by vacuum bagging process. The layer sheets are bonded using adhesive binding. The two specimens are joined together by simple welding process. The sheets are made with different combination of 1.1m thickness. The mechanical properties of base material and blank are listed in the table 1 and table 2.

Table 1. Mechanical properties of the layup materials

Properties	**Steel** (ST13)	**Aluminium (**AA1050)
Thickness, t (mm)	0.4& 0.7	0.4& 0.7
Youngs modulus, E(MPa)	210000	70000
Yield strength (MPa)	152	35
Tensile strength	282	75
Poisson ratio	0.3	0.31

Table 2. Mechanical properties of the blank materials

Material	Cast iron
Punch temperature	30 to 180^{0}C
Blank temperature	30 to 250^{0}C
Blank diameter	100mm
Punch diameter	50mm
Speed	60mm/min
Punch force	45 KN
Punch depth	24mm
Pressure	20bar
Coolant	Water

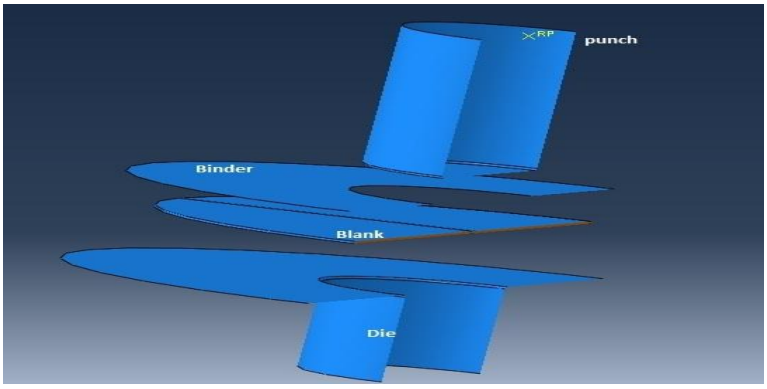

Figure 1. FE model (HMDD process)

Figure 1 shows the entire setup of the FEA model. The cup is produced by applying the load of 45KN force and depth 24mm. The force and depth are designed based on the key parameters such as tearing, earing, necking and wrinkling. Before beginning the procedure, the blank is electrochemically charged. The diameter of the blank is 100mm, punch diameter 50mm and speed 60mm/min. The gap of 1.2mm is fixed between blank holder and die. The experiment is carried out in an 80 ton hydraulic press. The pressure of the hydraulic press is 20bar. The pressure can be controlled by pressure valve control. The vibration is measured using vibrometer PSV-500. The measurement is carried out from the interval of 1000 to 5000Hz.

3. FE Simulation Process

The FE Abaqus/ explicit model were introduced to stimulate the multilayer sheet with HMDD at isothermal condition. The geomentry of the die and blank is made on CAD software and it is imported to Abaqus for solving. The tools and the blank are meshed with structural mesh with curved geomentry without formation of cracks. Die component is designed by R3D4 and the material properties of simulations are stated by Ladwik law by using the crucial parameters such as strain hardening, yield strength and ultimate tensile strength. Further, Hill criteria employed to find anisotropy coefficients at three different angles 0, 45 and 90^0. In addition to above, Arcelor V9 mode for forming limit curve is employed to predict the thinning of the base material. The anisotropy material is solved using 3D elesto plastic model. Symmetric boundary conditions applied throughout the specimen. The layers of Al and steel are defined by partitioning tool. The materials are assigned with different mechanical properties. This paper utilizes same hill quadratic expression used by Bagherzadeh et al [24] . The friction is coulomb and transient time is chosen by scaling scheme to reduce the simulation time. The friction coefficient is 0.1 for better forming process. The total simulation time for each case is 6hr on notebook with i7core processor. The oil pressure distribution model is another key parameter to yield proper forming process. Since the process is HMDD, the fluid pressure on the sheet is not uniform. To utilize the process with high accuracy Jensen et al proposed a mathematically model through Abaqus subroutine VD load. The next important step in FE simulation is choosing of failure criterion. There is various failure criteria used in FE model. Their theories are used to predict forming failure using FE modelling.

Fourier law of heat conduction can be written as [16-18],

$$\rho C_p \frac{\partial T}{\partial t} = \nabla.(K \nabla T) + q_v \quad (1)$$

Conduction of heat for the analytical solutions

$$\frac{\partial T}{\partial t} = \alpha \nabla^2 T \quad (2)$$

Temperature field

$$T = T_0 + \frac{q}{2\pi k R} e^{\frac{V(w+R)}{2\alpha}} \quad (3)$$

Gaussian distribution

$$q(r) = q_m e^{\frac{r^2}{2\sigma^2}} \quad (4)$$

The properties of the materials denoted by [19-20]

$$X_q(t) = \{x_q(t), y_q(t), z_q(t)\} \quad (5)$$

$$\phi(t, T) = \frac{q_m(t)}{\pi \rho(T) C_P(T) \sqrt{4\pi\alpha(T)}} \quad (6)$$

$$\overline{X_q}(t) = X - X_q(t) \quad (7)$$

$$\overline{x_q}(t) = x - x_q(t) \quad (8)$$

$$\overline{y_q}(t) = y - y_q(t) \quad (9)$$

$$\overline{z_q}(t) = z - z_q(t) \quad (10)$$

$$u = t - t^I \quad (11)$$

Determination of the temperature,

$$\theta(u, T) = \frac{u}{2\alpha(T)u + \sigma^2} \quad (12)$$

$$\alpha(T) = \alpha(T_0) \quad (13)$$

$$\frac{\partial T}{\partial t} = \nabla.(\alpha(T)\nabla T) \quad (14)$$

$$\hat{T}^0(X, t, T) \equiv T(X, t, T_0) \quad (15)$$

$$\hat{T}^{n+1}(X, t, T) \equiv \hat{T}(X, t, \hat{T}^n(x, t, T)) \quad (16)$$

$$\hat{T}(X, 0, T) \equiv T(X, t, T_0) \quad (17)$$

$$\hat{T}(X, t + \delta t, T) \equiv \hat{T}(X, t, T) \quad (18)$$

Modelling of the geometry

$$\psi_q(u,T) = \exp\left[\frac{\overline{x_q}u^2+\overline{y_q}u^2}{4\alpha(T)u+2\sigma^2} - \frac{\overline{Z_q}u^2}{4\alpha(T)u}\right] \quad (19)$$

$$\psi_m(u,T) = \exp\left[\frac{\overline{x_m}u^2+\overline{y_m}u^2}{4\alpha(T)u+2\sigma^2} - \frac{\overline{Z_m}u^2}{4\alpha(T)u}\right] \quad (20)$$

$$\hat{T}(X,t,T) = T_0 + \phi(t,T)\int_0^t \theta(u,T)[\psi_q(u,T) + f_d.f_c\psi_m(u,T)]du \quad (21)$$

$$f_d = \frac{\frac{dX_m(t)}{du}}{\frac{dX_q(t)}{du}} \quad (22)$$

$$f_c = \frac{\int_w q(w)}{\int_w q(x)} \quad (23)$$

$$\frac{dh(x)}{dt} = \begin{cases} \frac{\dot{m}}{\pi r t^2 \rho} & r(t) < r_{jet} \text{ and } \hat{T} \geq T_{melt} \\ 0 & \text{otherwise} \end{cases} \quad (24)$$

$$r(t) = \sqrt{\overline{x_q}t^2 + \overline{y_q}t^2} \quad (25)$$

4. Results and Discussion

4.1 Limiting drawing ratio

The LDR is the ratio, formation of maximum blank diameter without failure. LDR is used to estimate the formability of the sheets. The set of readings were calculated on both specimens at isothermal condition with HMDD. The 8 runs have been carried out totally. First four runs for non-isothermal model and others for isothermal model. From the earlier regards, the temperature of die/blank is always is always higher than punch. Hence the flow of material is very smooth into die cavity. In isothermal conditions, the cup is drawn between 105mm and 115mm diameter (LDR=2.1-2.5). The LDR is increased nearly 12% higher due to warm forming. Similar tests are run at non isothermal conditions.

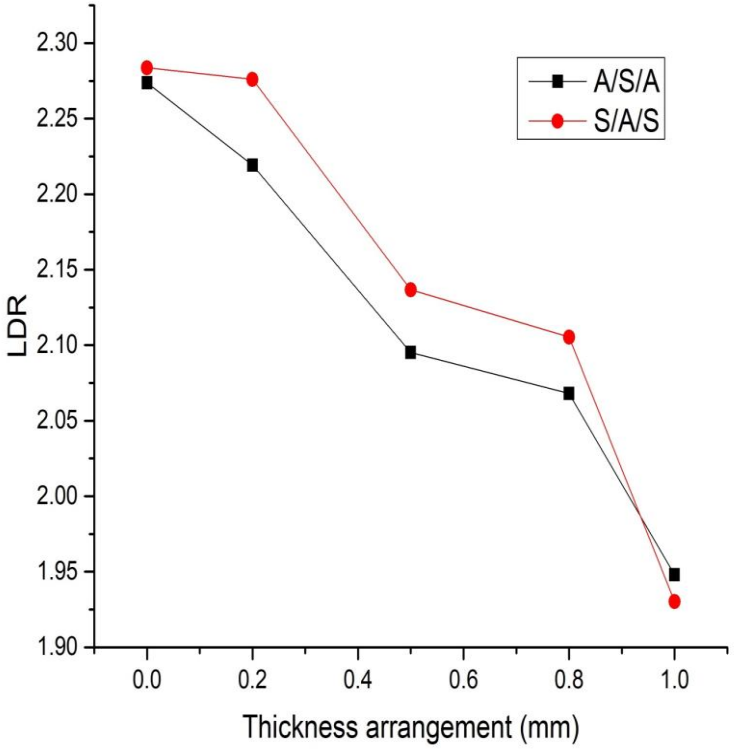

Figure 2. Limiting drawing ratio for various thickness arrangement

The cup height is improved for isothermal specimen than non-isothermal owing to the thermal conductivity of the specimen. To be precise, 22% average improvement in forming is witnessed for warm base plate than specimen at room condition, this perhaps due to higher temperature. Further, this sudden improvement is due to

the flow stress developed on the material at isothermal condition. On the contrary, the punch force required for S1 is higher than A1 owing to residual stress and reduction in flow stress due to higher punching displacement. Moreover, when the layup thickness is 0.4mm the LDR ratio for the isothermal is 4.5% higher than non-isothermal. Similar trend is reported by Bagherzadeh et al and Zhu et al [14,25]. As the thickness of the arrangement is higher, the LDR of the both specimen is very identical.

4.2 Effect of layer arrangement

The nose like curve is obtained to predict the fluid pressure and drawing ratio. The indication of nose in figure represents the successful formation of LDR in multilayer sheet.

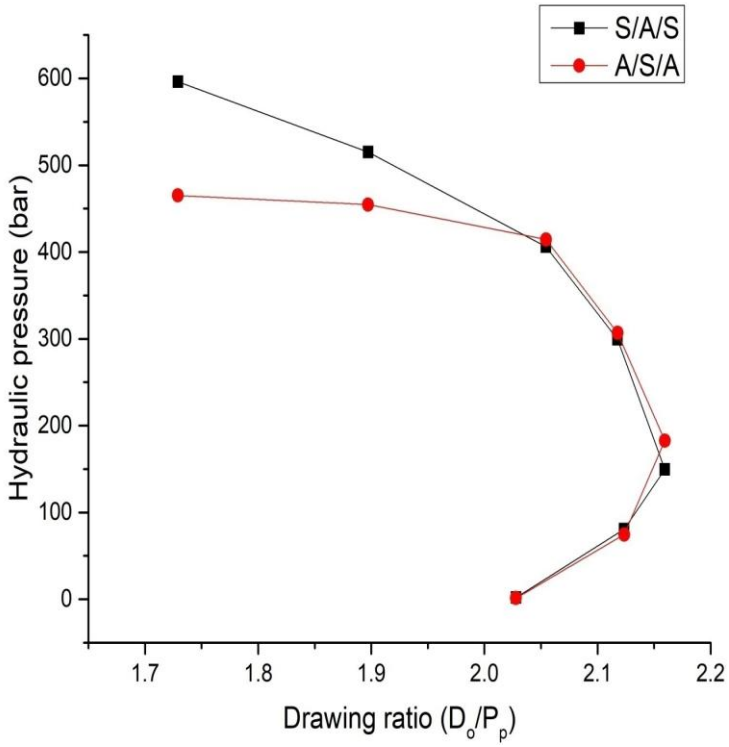

Figure 3. Effect of hydraulic pressure for different drawing ratio

Figure 3, shows the prediction of LDR for different layups. The figure predicts the thickness distribution of each layer. The thickness of S/A/S layup is lower than A/S/A due to the direct contact of the punch to the weakest material. In addition to above, higher friction coefficient also responsible for the above regards. Simultaneously, the reduction of thickness in the layer of A/S/A is 5% higher than S/A/S layup[26]. More thicken leads to wrinkling of A/S/A sheets. Hence to avoid the tearing it is recommended to use S/A/S than A/S/A layup. As the drawing ratio increases, the both curves come identical to each other after 2.01 of drawing ratio.

4.3 Effect on temperature variation on thickness / strain

Understanding of thickness distribution is a significant factor since it defines the formation of tearing. Excess thinning leads to tearing of specimen and high thickness affects the product life. To analyse the thinning, the cup is formed on the both specimens at isothermal and non-isothermal conditions in presence of HDMR.

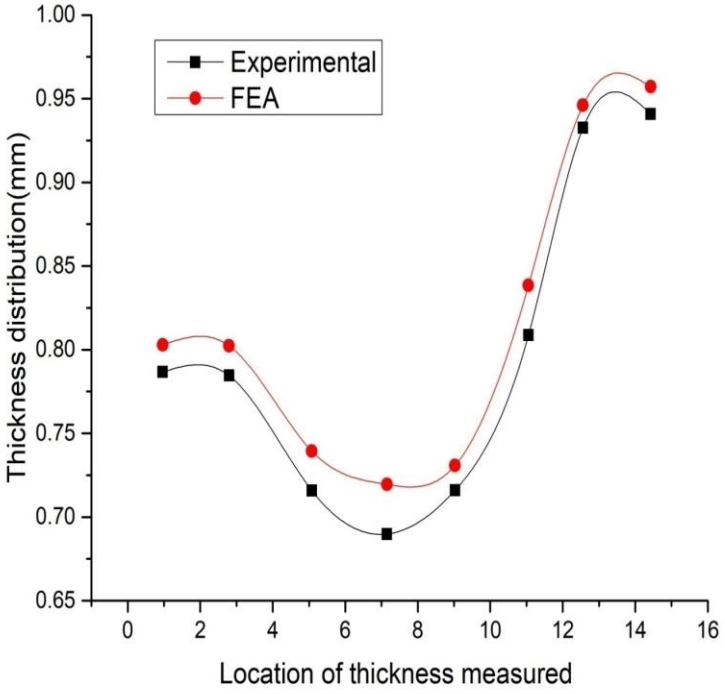

Figure 4. Thickness distribution for different locations for isothermal specimen

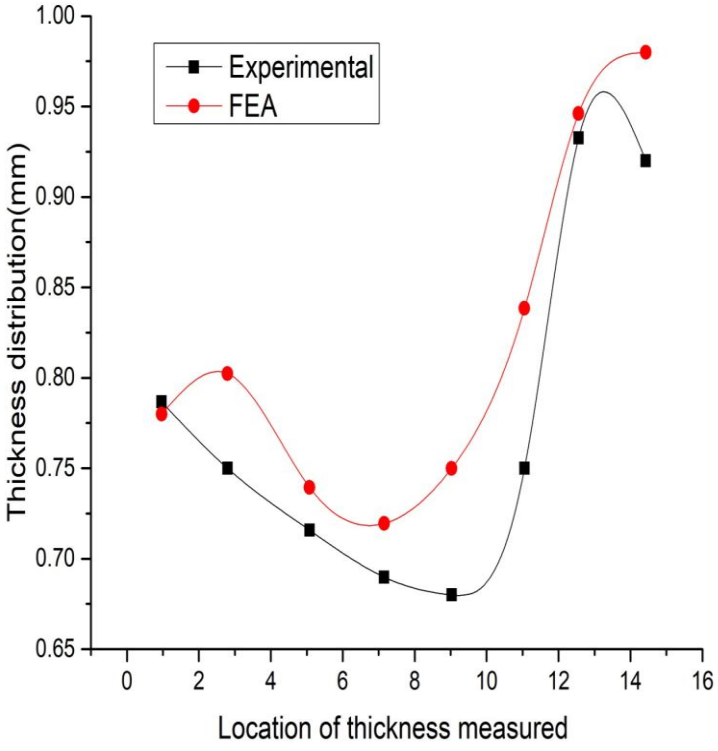

Figure 5. Thickness distribution for different locations for non-isothermal specimen

Figure 4 and 5 shows the thickness distribution of the cup at different locations of the flange. For isothermal specimen forming, the thickness is constant due to the balance between punch and model. The thickness of the sheet decreased and reached value of 0.95mm. For the A1 specimen, the thickness is maximum at the location is 0.845mm. The failure occurs at the die corner. From the above consideration it is evident that, the thinning can be reduced by lowering the flow stress at high temperature than room temperature [27]. Although two specimens are different but the curves which predicts thickness distribution is only little significant.

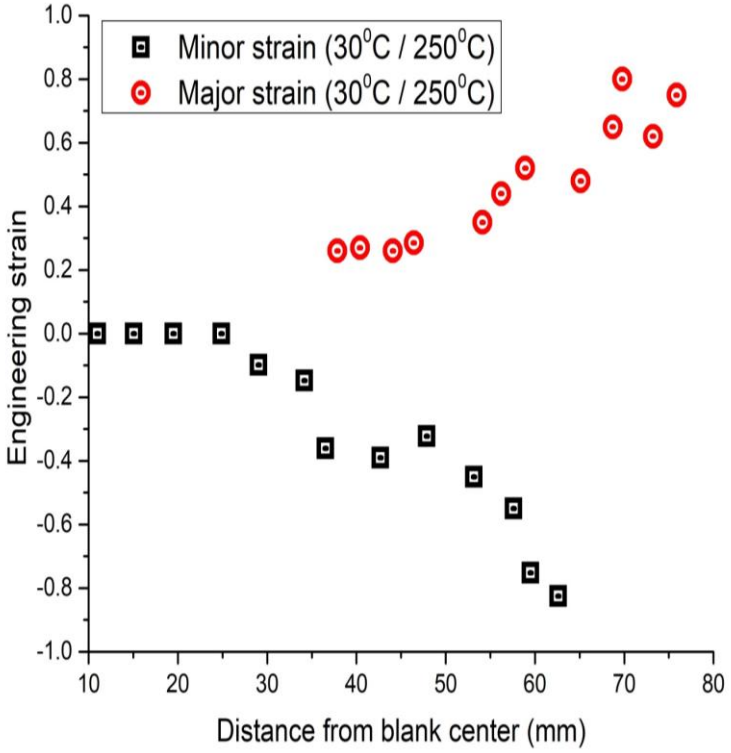

Figure 6. Major and minor strain distributions for isothermal forming

Figure 6 shows the strain generated due to change in distance from blank. Until the distance of 30mm, the both strains are unique upto the blank distance 40mm.

4.4 Effect of FRF based on forming simulation

The FRF is obtained from formulation of both sides of the blank. The point 1 indicates the sheet of A/S/A and point 2 indicates the blank made of S/A/S. The natural frequencies and the error % is reported in the table. The error % is higher as the frequency is higher[28]. The FRF computation is done on both symmetry points which are chosen by superposing FEM mesh.

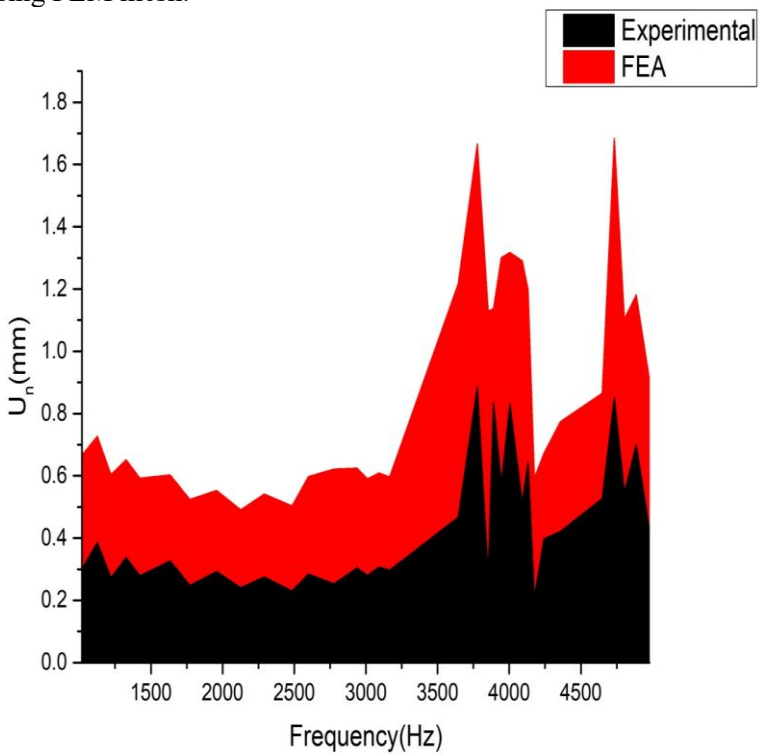

Figure 7. Natural frequency variation for A1 specimen

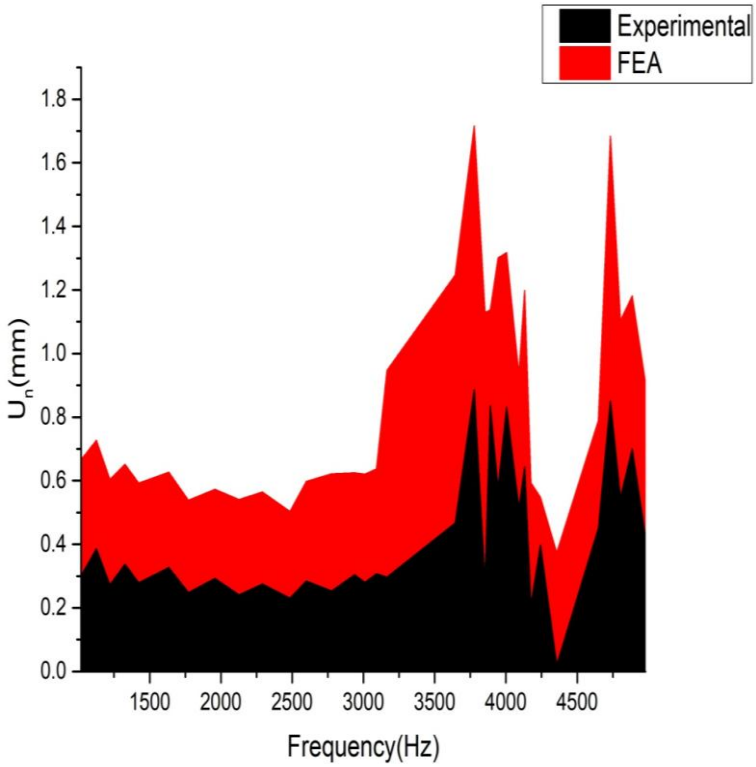

Figure 8. Natural frequency variation for S1 specimen

From figure 7 and 8 it is evident that Un is higher as the natural frequency is beyond 3500Hz, there is an drastic change in Un. Further, it is very fascinating to witness Un is identical for both the conditions. However, the frequency observed by the isothermal is slightly lower than non-isothermal owing the plastic strain.

4.5 Effect of punch force

The HMDD of the multilayer sheet at different drawing ratios, punch stroke and pressure of fluid simulated and compared with experimental values. Figure compares the forming force with punch stroke.

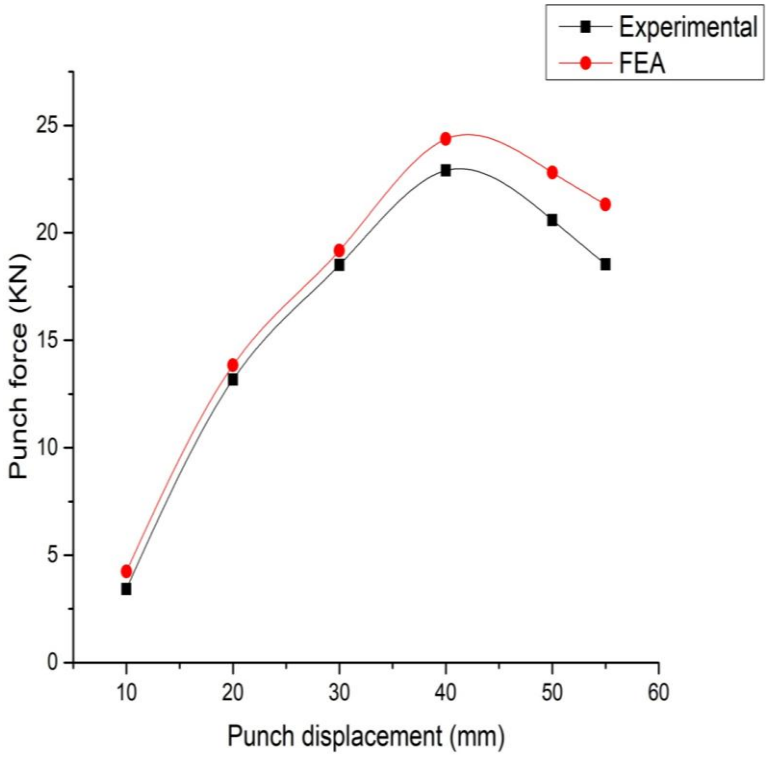

Figure 9. Displacement of punch force for various displacement for A1 specimen

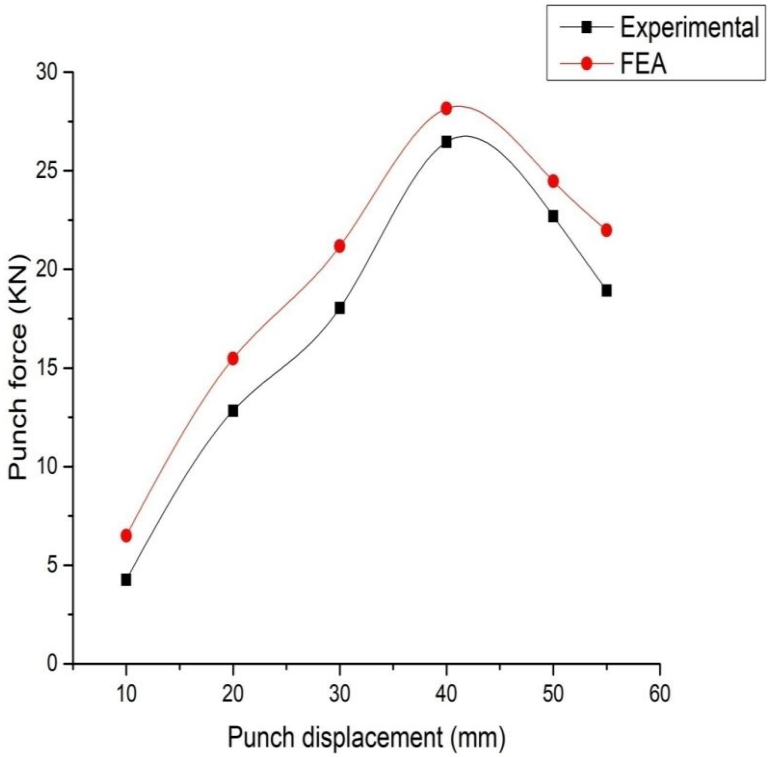

Figure 10. Displacement of punch force for various displacements for S1

The A/S/A layup of thickness 0.4/0.7/0.4 and S/A/S of 0.4/0.7/0.4 respectively. the overall forming force is presented in the figure 9 and 10 for both model. It is evident that, isothermal specimen requires lesser punch force compared to non-isothermal owing to the mechanical properties and heating effect on layer thickness. Further, the total force required for 40mm displacement for with and without base material heating are 23KN and 26KN respectively. Hence 13% of lesser punch force is sufficient for isothermal specimen to complete the task compared to non-isothermal[29]. The uncertainty between the experimental and the numerical validation is falls in acceptable limit.

4.6 Failure theories

The failure theories of the model were detected at different locations of the cup. Especially near punch corner and near flange. These failures were reported when DR value is above 2.3. Similar theories were reported by Bang et al. The failure of the A1 and S1 specimens are also represented in FEA approach. In A1 specimen, most failures formed at the upper region of the wall. The failures were due to brittle nature of structures at room temperature and high tensile stress at wall, high strain rate and wrinkling[15].

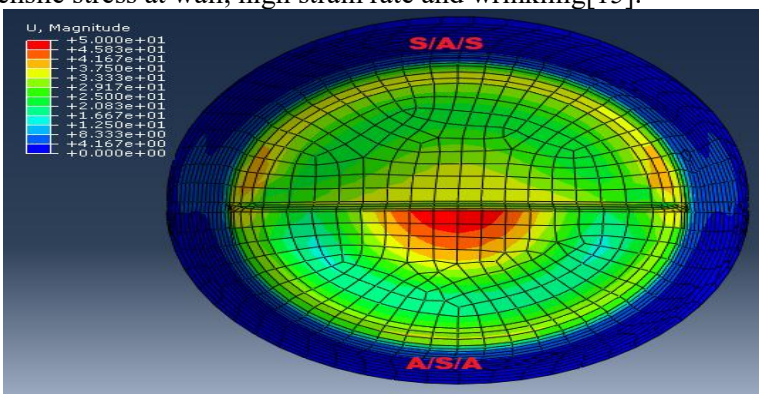

Figure 11. Displacement simulation for the multi-layer blank at initial stage

Figure 11- 15 shows the behaviour of the base material during machining. The formation of the thinning is higher for the S/A/S blank is higher than A/S/A due to the different yield strength.

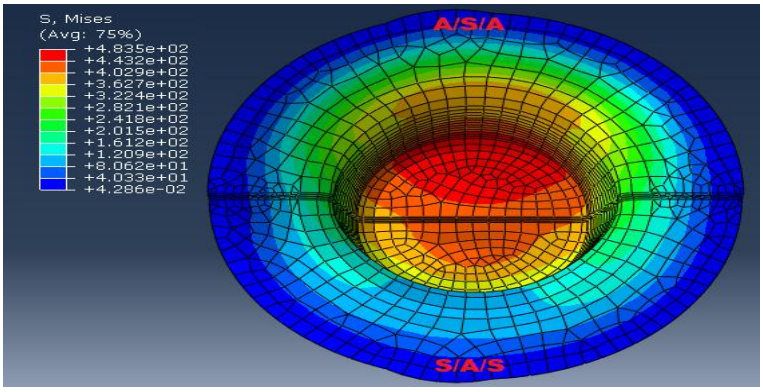

Figure 12. Stress distribution for the multi-layer blank after forming

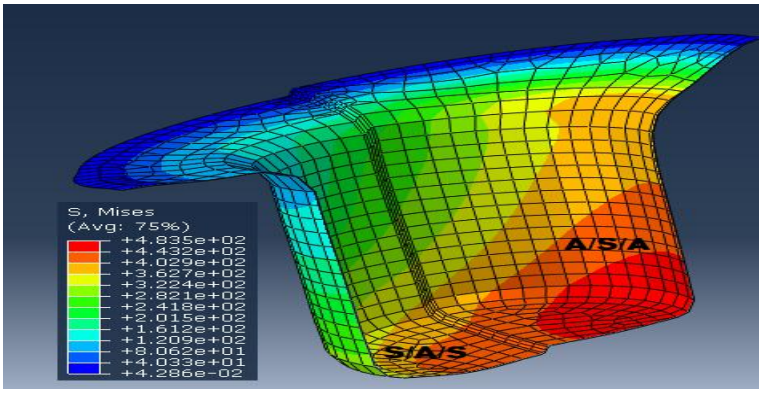

Figure 13. Cross sectional view of stress distribution for the multi-layer blank after forming

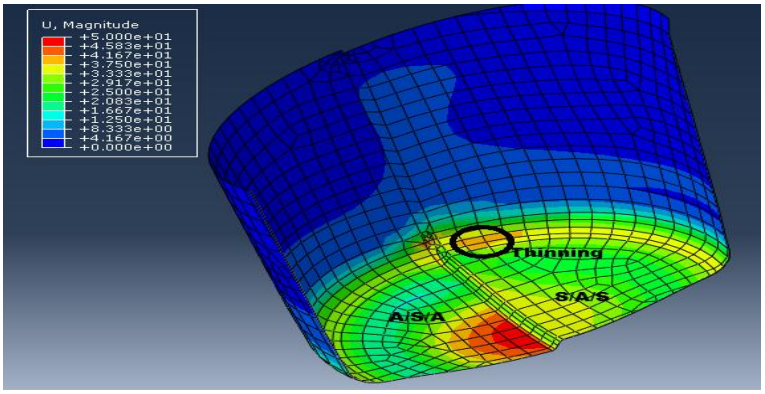

Figure 14. Surface cracks developed on the flange surface due to high strain after thinning

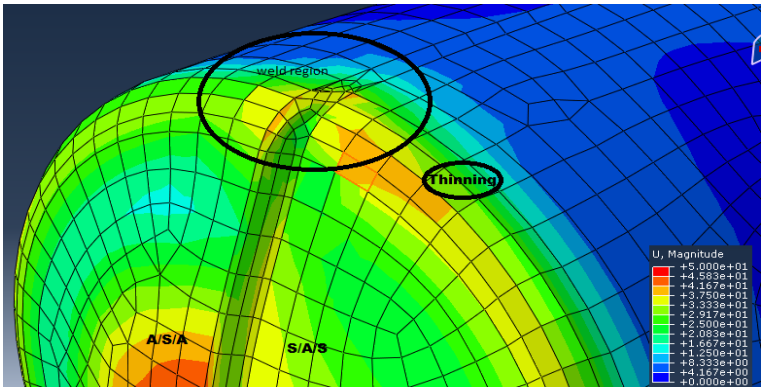

Figure 15. Surface cracks developed on the welded region due to high strain after thinning

Further, formation of thinning leads to crack on the weld as the punch force is high. On the other hand, the total stress distribution for the A/S/A is higher than S/A/S due to the layer thickness and layup configurations.

4.7 Effect of thickness and inner diameter of polyurethane ring

Figure depicts the behavior of cross-sectional dimensions of poly-urethane ring subjected to compression loading ratio of 10%. It is evident from the figure, up to d_t/d_i= 1.0, the inner diameter reaches to maximum level and the height of the cup increases at the same point.

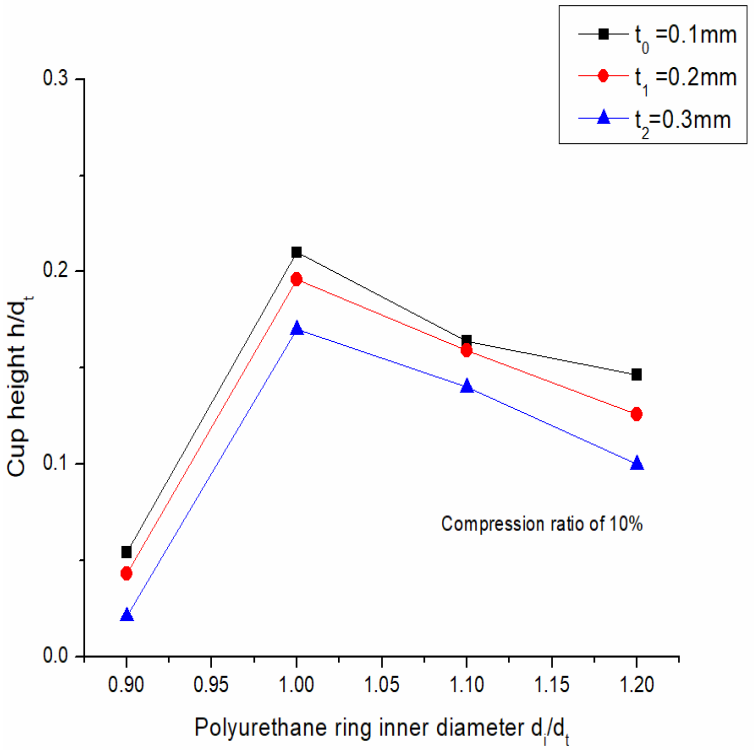

Figure 16. Behaviour of polyurethane ring inner diameter on cup height

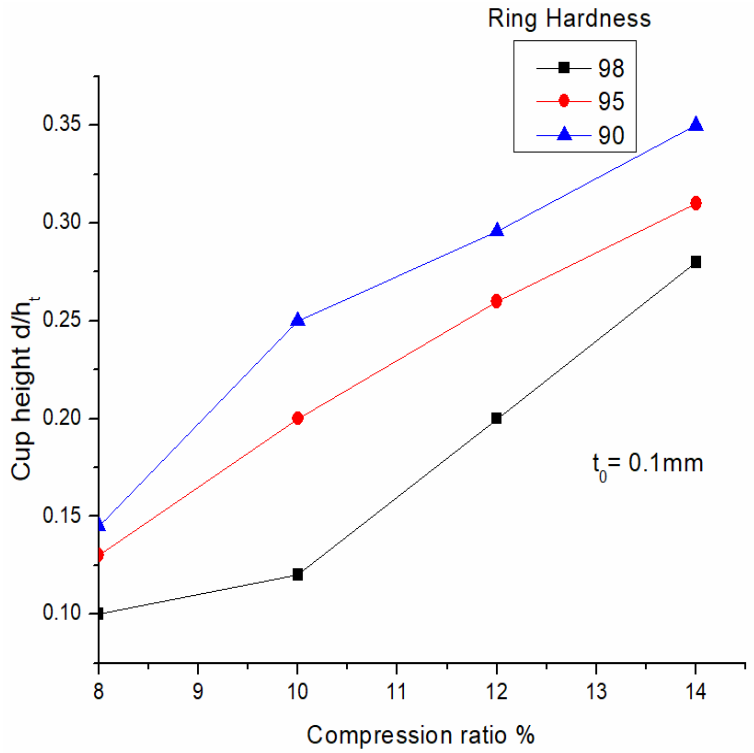

Figure 17. Behaviour of ring on different compression ratio for t_0=0.1mm

Beyond the ratio, ring diameter increases with decreasing the height of cup. Minor deformations occur in the profile section particularly when the thickness of the blank is very small. Cracks will appear in the profile section, when the $d_t/d_i \leq 1.0$ and the forces are punching up around the die of polyurethane ring as explained by M.A.Hassan et.al. The recommended polyurethane inner ring diameter was found to be $d_t=1.0d_i$ and the maximum compression loading ratio was limited to 10% in order to avoid the formation of cracks in the cup region for about three drawing operations. Beyond three operations, the loading ratio can be increased up to maximum of 25%.

4.8 Hardness of polyurethane ring:

The hardness of the polyurethane ring can be investigated under variable loading ratio.

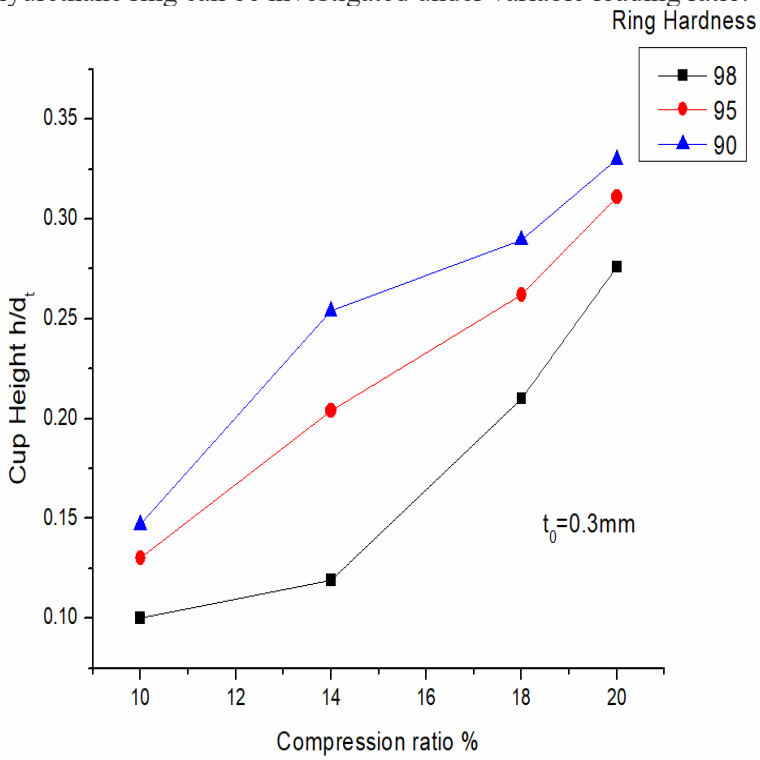

Figure 18. Behaviour of ring on different compression ratio for t_0=0.3mm

Figure depicts the experimental analysis of various blank thickness of varying sizes 0.1mm and 0.3mm respectively. As stated earlier, maximum compression loading ratio was limited to 10% up to three drawing operations. The calculated height of cup was depicted in the figure after third drawing process. The interfacial force developed between blank and ring rises with higher hardness value of ring. The polyurethane ring made of softer material achieves more cup height as compared with ring made of harder material.

5. Conclusion

In this research, the dynamic simulation of deep drawing is carried out on HMDD of A/S/A and S/A/S multilayer sheets to predict the parameters ensuring the formation of cup without failure. Experimental and numerical approaches had been considered and compared to each other for validation and found that experiments are in good agreement with FE model. The results are drawn as follows

- The LDR for the isothermal condition is improved 12% compared to room temperature. Further, the LDR of non isothermal is improved 9% higher than isothermal forming.
- The deformation characteristics are predicted by comparing the thickness distribution for both temperature gradient conditions. At isothermal conditions, thinning takes place at 25mm from the bottom with minimum thickness is 0.82mm. Similarly, at non isothermal the thickness is close enough to the above as 0.82mm.

- The Eigen frequency and forces are compared. The experimental measured natural frequencies are used to predict the dynamic behaviour of laminate sheet. Higher frequencies higher error owing to high intense of material flow.
- The implementation of HMDD with desirable fluid pressure yields higher forming. The formability of S/A/S and A/S/A is significant compared to conventional DD. The favourable hydraulic pressure avoids the failure of the material.
- It is found that, optimum drawing ratio significantly decreases the critical pressure which leads to the extension of safe working limit. This is achievable by obtaining the favourable fluid pressure
- The safe working zone of the layup A/S/A is lower than S/A/S owing to the HDR and LDR. In addition, the limiting of A/S/A is compulsory due to the thinning of layer at wall region.

Nomenclature

q_V	volumetric heat source term
q	total heat input
q_m	distributed heat source peak magnitude
σ	distributed heat source size parameter
v	heat source velocity
r	distance from heat source
ρ	density
c_p	specific heat capacity
k	thermal conductivity
α	thermal diffusivity
T_o	ambient temperature
t	time
t′	time of heat application
zb^t	is the z-coordinate

References

1) Fan JP, Tang CY, Tsui CP, Chan LC, Lee TC. 3D finite element simulation of deep drawing with damage development. Int J Mach Tools Manuf 2006. https://doi.org/10.1016/j.ijmachtools.2005.07.044.
2) Padmanabhan R, Oliveira MC, Alves JL, Menezes LF. Influence of process parameters on the deep drawing of stainless steel. Finite Elem Anal Des 2007. https://doi.org/10.1016/j.finel.2007.06.011.
3) Kadkhodayan M, Afshin E. Thinning behavior of laminated sheets metal in warm deep-drawing process under various grain sizes. MATEC Web Conf 2016. https://doi.org/10.1051/matecconf/20168015001.
4) Hosford WF, Caddell RM. Metal forming: Mechanics and metallurgy. 2011. https://doi.org/10.1017/CBO9780511976940.
5) Parsa MH, Yamaguchi K, Takakura N. Redrawing analysis of aluminum-stainless-steel laminated sheet using FEM simulations and experiments. Int J Mech Sci 2001. https://doi.org/10.1016/S0020-7403(01)00038-8.
6) Tseng HC, Hung C, Huang CC. An analysis of the formability of aluminum/copper clad metals with different thicknesses by the finite element method and experiment. Int J Adv Manuf Technol 2010. https://doi.org/10.1007/s00170-009-2446-4.
7) Manigandan S, Gunasekar P, Nithya S, Devipriya J, Saravanan WSR, Venkatesan S. Acoustic and vibration analysis of pineapple leaf fibre laminates for aircraft applications. Int J Ambient Energy 2018. https://doi.org/10.1080/01430750.2018.1530138.
8) Singh SK, Gupta AK, Mahesh K. A study on the extent of ironing of EDD steel at elevated temperature. CIRP J Manuf Sci Technol 2010. https://doi.org/10.1016/j.cirpj.2010.07.002.
9) van den Boogaard AH, Bolt PJ, Werkhoven RJ. Modeling of AlMg Sheet Forming at Elevated Temperatures. Int J Form Process 2007. https://doi.org/10.3166/ijfp.4.361-375.
10) Zheng K, Zhu L, Lin J, Dean TA, Li N. An experimental investigation of the drawability of AA6082 sheet under different elevated temperature forming processes. J Mater Process Technol 2019. https://doi.org/10.1016/j.jmatprotec.2019.05.006.
11) Takuda H, Mori K, Masuda I, Abe Y, Matsuo M. Finite element simulation of warm deep drawing of

aluminium alloy sheet when accounting for heat conduction. J Mater Process Technol 2002. https://doi.org/10.1016/S0924-0136(01)01180-3.
12) Morovvati MR, Fatemi A, Sadighi M. Experimental and finite element investigation on wrinkling of circular single layer and two-layer sheet metals in deep drawing process. Int J Adv Manuf Technol 2011. https://doi.org/10.1007/s00170-010-2931-9.
13) Mashayekhi M, Dehghani F, Torabian N, Salimi M. An experimental and numerical study of ductile fracture of copper/stainless steel clad sheet in deep drawing process. Iran J Sci Technol - Trans Mech Eng 2015.
14) Bagherzadeh S, Mirnia MJ, Mollaei Dariani B. Numerical and experimental investigations of hydro-mechanical deep drawing process of laminated aluminum/steel sheets. J Manuf Process 2015. https://doi.org/10.1016/j.jmapro.2015.03.004.
15) Kim JB, Yoon JW, Yang DY, Barlat F. Investigation into wrinkling behavior in the elliptical cup deep drawing process by finite element analysis using bifurcation theory. J Mater Process Technol 2001. https://doi.org/10.1016/S0924-0136(01)00504-0.
16) Mayavan T, Karthikeyan L, Senthilkumar VS. Experimental and Numerical Studies on Isothermal and Non-isothermal Deep Drawing of IS 513 CR3 Steel Sheets. J Mater Eng Perform 2016. https://doi.org/10.1007/s11665-016-2325-8.
17) Jalali Aghchai A, Shakeri M, Mollaei Dariani B. Influences of material properties of components on formability of two-layer metallic sheets. Int J Adv Manuf Technol 2013. https://doi.org/10.1007/s00170-012-4368-9.
18) Maleki H, Bagherzadeh S, Mollaei-Dariani B, Abrinia K. Analysis of bonding behavior and critical reduction of two-layer strips in clad cold rolling process. J Mater Eng Perform 2013. https://doi.org/10.1007/s11665-012-0342-9.
19) Lang L, Danckert J, Nielsen KB. Multi-layer sheet hydroforming: Experimental and numerical investigation into the very thin layer in the middle. J Mater Process Technol 2005. https://doi.org/10.1016/j.jmatprotec.2005.06.033.
20) Fazli A, Dariani BM. Parameter study of the axisymmetric hydromechanical deep drawing process. Proc Inst Mech Eng Part B J Eng Manuf 2006. https://doi.org/10.1243/09544054JEM672.
21) Rahmani F, Hashemi SJ, Moslemi Naeini H, Deylami Azodi H. Numerical and experimental study of the efficient parameters on hydromechanical deep drawing of square parts. J Mater Eng Perform 2013. https://doi.org/10.1007/s11665-012-0301-5.
22) Choi H, Koç M, Ni J. A study on the analytical modeling for warm hydro-mechanical deep drawing of lightweight materials. Int J Mach Tools Manuf 2007. https://doi.org/10.1016/j.ijmachtools.2006.12.005.
23) Zhang R, Lang L, Zafar R, Lin L, Zhang W. Investigation into thinning and spring back of multilayer metal forming using hydro-mechanical deep drawing (HMDD) for lightweight parts. Int J Adv Manuf Technol 2016. https://doi.org/10.1007/s00170-015-7415-5.
24) Bagherzadeh S, Mollaei-Dariani B, Malekzadeh K. Theoretical study on hydro-mechanical deep drawing process of bimetallic sheets and experimental observations. J Mater Process Technol 2012. https://doi.org/10.1016/j.jmatprotec.2012.04.002.
25) Huiwen Z, Baoyi Y, Li Z, Jingkai C, Boning Y, Shuning L, et al. Deformation mechanism of blank holder area in deep drawing process for AZ31 magnesium alloy. Mater Res Express 2019. https://doi.org/10.1088/2053-1591/aafa43.
26) Safdarian R, Pournouri H. Experimental and numerical study of hydro-mechanical deep drawing of 2024 aluminum alloy sheet at elevated temperatures. Mater Res Express 2019. https://doi.org/10.1088/2053-1591/ab1ae5.
27) Rebeyka CJ, Button ST, Lajarin SF, Marcondes PVP. Mechanical behavior of HSLA350/440 and DP350/600 steels at different temperatures and strain rates. Mater Res Express 2018. https://doi.org/10.1088/2053-1591/aac874.
28) Horiike N, Yoshihara S, Tsuji Y, Okude Y. Effect of Blank Holder Force with Low Frequency Vibration Technique in Circular-Cup Deep-Drawing Using AZ31 Magnesium Alloy Sheet. Adv Mater Res 2012. https://doi.org/10.4028/www.scientific.net/amr.433-440.666.
29) Modanloo V, Gorji A, Bakhshi-Jooybari M. Effects of forming media on hydrodynamic deep drawing. J Mech Sci Technol 2016. https://doi.org/10.1007/s12206-016-0433-x.